Journal of Molecular Catalysis A: Chemical 344 (2011) 18–27

Contents lists available at ScienceDirect

Journal of Molecular Catalysis A: Chemical

journal homepage: www.elsevier.com/locate/molcata

Synthesis, characterization and catalytic activities of vanadium complexes containing ONN donor ligand derived from 2-aminoethylpyridine

Mannar R. Maurya[a,*], Manisha Bisht[a], Fernando Avecilla[b]

[a] Department of Chemistry, Indian Institute of Technology Roorkee, Roorkee 247667, India
[b] Departamento de Química Fundamental, Universidade da Coruña, Campus de A Zapateira, 15071 A Coruña, Spain

ARTICLE INFO

Article history:
Received 15 February 2011
Received in revised form 23 April 2011
Accepted 25 April 2011
Available online 7 May 2011

Keywords:
Vanadium complexes
Encapsulated complex
Catalytic activity
Oxidation of styrene
Oxidation of cyclohexene
Oxidation of organic sulfides

ABSTRACT

Reaction between $[V^{IV}O(acac)_2]$ and the ONN donor Schiff base Hpydx-aepy (**I**) (Hpydx-aepy = Schiff base obtained by the condensation of pyridoxal and 2-aminoethylpyridine) resulted in the formation of a complex $[V^{IV}O(acac)(pydx\text{-}aepy)]$ **(1)**. Addition of aqueous 30% H_2O_2 to 1 yields the poor stable oxidoperoxidovanadium(V) complex $[V^{V}O(O_2)(pydx\text{-}aepy)]$ **(2)**. Its formation has also been demonstrated in solution by treating 1 with H_2O_2 in methanol. Reaction of vanadium exchanged zeolite-Y with I in methanol followed by aerial oxidation gave zeolite-Y encapsulated dioxidovanadium(V) complex, abbreviated as $[V^{V}O_2(pydx\text{-}aepy)]$-Y **(4)**. The crystal and molecular structure of **1** has been determined, confirming the ONN binding mode of the ligand. The encapsulated complex $[V^{V}O_2(pydx\text{-}aepy)]$-Y **(4)** catalyses the oxidation of styrene, cyclohexene, methyl phenyl sulfide and diphenyl sulfide using H_2O_2 as oxidant in good yield. Styrene under optimised reaction conditions gave four reaction products namely, styrene oxide, benzaldehyde, 1-phenylethane-1,2-diol and benzoic acid while organic sulfides gave the corresponding sulfoxide as the major product. Cyclohexene gave cyclohexene epoxide, 2-cyclohexene-1-one, 2-cyclohexene-1-ol and cyclohexane-1,2-diol. Neat complex $[V^{IV}O(acac)(pydx\text{-}aepy)]$ has been used as catalyst precursor to compare its catalytic activities with the encapsulated one.

1. Introduction

Modeling the structure and properties of vanadium-containing bio-molecules has influenced research on vanadium coordination chemistry. Vanadate-dependent haloperoxidases (V-HPOs) are important examples amongst bio-molecules in this context [1–5]. Vanadium haloperoxidases not only catalyse the oxidative halogenation, they accelerate the oxidation of aliphatic as well as aromatic substrates in the presence of hydrogen peroxide, organic hydroperoxides or molecular oxygen [6–10]. Several models and other vanadium complexes have been shown to catalyse all these reactions as well [4–14]. Solution studies on model complexes have also been performed to provide knowledge on the understanding of the role of enzymes and mechanism of the catalytic reactions [10–14]. We reported structural and functional models of VHPO considering benzimidazole and imidazole derived ligands [11,12] and have explored their catalytic potential for the oxidation of styrene, benzoin, methyl phenyl sulfide and diphenyl sulfide. Encapsulation of such complexes in nano-cavities of zeolite-Y not only improved its catalytic activity with high turn over frequency but catalyst also became recyclable for further use [15]. The advantages of immobilised metal complexes promoted several research groups to investigate the catalytic properties of various metal complexes entrapped within the nano-cavities of zeolite-Y [16–25].

In this paper, we describe the synthesis and characterization of oxidovanadium(IV) complex of ligand **I** (Scheme 1). Its reactivity with H_2O_2 has also been described. Dioxidovanadium(V) complex has been encapsulated in the nano cavity of zeolite-Y and its catalytic activity has been demonstrated considering the oxidation, by peroxide, of styrene, cyclohexene, methyl phenyl sulfide and diphenyl sulfide. For comparison, we have used oxidovanadium(IV) complex as catalyst precursor and tested for all the above reactions.

2. Experimental

2.1. Materials and methods

V_2O_5, $VOSO_4{\cdot}5H_2O$ (Loba Chemie, Mumbai, India), acetylacetone (Hacac) (Aldrich, U.S.A.), pyridoxal hydrochloride, cyclohexene (Himedia, India), methyl phenyl sulfide (Alfa Aesar, U.S.A.), styrene and 2-(2-aminoethyl)pyridine (Acros Organics, U.S.A.), 30% aqueous H_2O_2 (Qualigens, India) were used as obtained. Zeolite-Y (Si/Al = ca. 10) was obtained as gift from National Chemical

* Corresponding author. Tel.: +91 1332 285327; fax: +91 1332 273560.
E-mail address: rkmanfcy@iitr.ernet.in (M.R. Maurya).

1381-1169/$ – see front matter © 2011 Elsevier B.V. All rights reserved.
doi:10.1016/j.molcata.2011.04.017

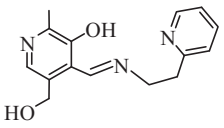

Hpydx-aepy (**I**)

Scheme 1.

laboratory, Pune, India. All other chemicals and solvents used were of AR grade. [VO(acac)$_2$] was prepared according to method reported in the literature [26].

Elemental analyses of the ligand and complexes were obtained by an Elementar model Vario-EL-III. IR spectra were recorded as KBr pellets on a Nicolet 1100 FT-IR spectrometer after grinding the sample with KBr. Electronic spectra of ligand and complexes were recorded in methanol or DMF. Electronic spectrum of zeolite-Y encapsulated complex was recorded in Nujol using Shimadzu 1601 UV–vis spectrophotometer by layering the mull of the sample to inside of one of the cuvettes while keeping the other one layered with Nujol as reference. ^{51}V NMR spectrum of peroxo complex was recorded on a Bruker Avance 400 MHz spectrometer with the common parameter settings in DMSO-d$_6$. δ(^{51}V) values are quoted relative to $VOCl_3$ as external standard. X-ray powder diffractograms of zeolite containing samples were recorded using a Bruker AXS D8 advance X-ray powder diffractometer with a Cu Kα target. Scanning electron micrographs (SEMs) of samples were recorded on a Leo instrument model 435VP. The samples were dusted on alumina and coated with thin film of gold to prevent surface charging and to protect the surface material from thermal damage by electron beam. In all analyses, a uniform thickness of about 0.1 mm was maintained. A constant voltage of 20 kV was applied so that only outer surface of the zeolite-Y was accessible. Magnetic susceptibility of oxidovanadium(IV) complex was determined at 298 K with a Vibrating Sample Magnetometer model 155, using nickel as a standard and diamagnetic corrections were done with Pascal's constants [27]. A Thermo Nicolet gas chromatograph with a HP–1 capillary column (30 m × 0.25 mm × 0.25 μm) was used to analyse the reaction products. The identity of the products was confirmed using a GC–MS model Perkin-Elmer, Clarus 500 by comparing the fragments of each product with the library available.

2.2. Preparations

2.2.1. Preparation of Hpydx-aepy (*I*)

Pyridoxal hydrochloride (0.406 g, 2 mmol) was dissolved in absolute methanol (15 ml) in the presence of KOH (0.112 g, 2 mmol) with stirring. After 1 h of stirring, the separated white solid (KCl) was filtered and the obtained clear solution was added to a solution of 2-(2-aminoethyl)pyridine (0.244 g, 2 mmol) in methanol (15 ml) with stirring and the resulting reaction mixture was refluxed for 2 h. The volume of solvent was reduced to ca. 10 ml and in situ formed yellow-orange ligand was used as such for further reaction.

2.2.2. Preparation of [$V^{IV}O$(acac)(pydx-aepy)] (*1*)

A solution of in situ generated Hpydx-aepy (equivalent to 2 mmol) as mentioned above in dry methanol (10 ml) was treated with [$V^{IV}O(acac)_2$] (0.530 g, 2 mmol) dissolved in dry methanol (10 ml) and the resulting reaction mixture was refluxed on a water bath for 3 h. After cooling to room temperature and adding distilled water (10 ml), the flask was kept at room temperature for ca. 10 h. The separated brown crystals of **1** were filtered off, washed with methanol (10 ml) and dried in vacuum over silica gel at room temperature. Yield: 0.65 g (86.0%). *Anal.* Calc. for $C_{20}H_{23}N_3O_5V$ (436.4): C, 55.1; H, 5.3; N, 9.6. Found: C, 55.0; H, 5.4; N, 9.4%.

2.2.3. Preparation of [$V^{V}O(O_2)$(pydx-aepy)] (*2*)

Complex [$V^{IV}O$(acac)(pydx-aepy)] (0.872 g, 2 mmol) was dissolved in 40 ml of hot methanol and cooled to room temperature after filtration. An aqueous 30% H_2O_2 (2 ml dissolved in 5 ml of methanol) was added drop wise to the above solution within 15 min under stirring. Stirring was continued where yellow solid slowly separated out within 30 min. This was filtered off, washed with methanol and dried in vacuo. This complex is poor stable (it looses oxygen at room temperature) and therefore only IR, electronic and ^{51}V NMR spectra could be recorded with the sample. Yield: 0.650 g (75%). ^{51}V NMR (DMSO-d$_6$, δ/ppm): −497 (minor) and −519 (major).

2.2.4. Preparation of [$V^{IV}O$]-Y (*3*)

A filtrated solution of $VOSO_4.5H_2O$ (9.0 g, 36 mmol) dissolve in 100 ml of distilled water was added to a suspension of Na-Y zeolite (15.0 g) in 900 ml of distilled water and the reaction mixture was heated at 90 °C with stirring for 24 h. The light bluish solid was filtered, washed with hot distilled water until filtrate was free from any vanadyl ion content and dried at 150 °C for 12 h. Yield: 14.9 g (99.2%). Found: V (ICP-MS), 4.6%.

2.2.5. Preparation of [$V^{V}O_2$(pydx-aepy)]-Y (*4*)

[$V^{IV}O$]-Y (3.0 g) and Hpydx-aepy (prepared in situ from 5 mmol each of pyridoxal and 2-aminoethyl pyridine) were mixed in methanol (50 ml) and the reaction mixture was heated under reflux for 14 h in an oil bath with stirring. The resulting material was filtered and then Soxhlet extracted with methanol to remove unreacted ligand. It was finally treated with hot DMF while stirring for 1 h, filtered, washed with DMF followed by hot methanol. The uncomplexed metal ions present in the zeolite were removed by stirring with aqueous 0.01 M NaCl (150 ml) for 10 h. The resulting greenish-yellow solid was filtered, washed with hot methanol followed by distilled water until no precipitate of AgCl was observed in the filtrate on treating with $AgNO_3$. The solid was further suspended in methanol and oxidised by passing air while stirring at room temperature for 24 h. Finally the obtained cream solid was dried at 120 °C for several hours. Yield: 2.3 g (76.7%). Found: V (ICP-MS), 2.6; N, 2.2%.

2.3. Crystal structure determination

Three-dimensional X-ray data for 1 H_2O were collected on a Bruker SMART Apex CCD diffractometer at 153(2) K, using a graphite monochromator and Mo–K$_\alpha$ radiation (λ = 0.71073 Å) by the ϕ–ω scan method. Reflections were measured from a hemisphere of data collected of frames each covering 0.3° in ω. Of the 19025 reflections measured, all of which were corrected for Lorentz and polarization effects, and for absorption by semi-empirical methods based on symmetry-equivalent and repeated reflections, 2894 independent reflections exceeded the significance level $|F|/\sigma(|F|) > 4.0$. Complex scattering factors were taken from the program package SHELXTL [28]. The structure was solved by direct method and refined by full-matrix least-squares method on F^2. The non-hydrogen atoms were refined with anisotropic thermal parameters in all cases. The hydrogen atoms were placed in idealised positions and refined by using a riding mode, except the hydrogen atoms from the water molecule, two hydrogen atoms of carbon atoms and the hydrogen atom from the hydroxyl group. One hydrogen atom (H1WB) and the hydrogen atom of the hydroxyl group (H_2O) were located from a difference electron density map and fixed to the oxygen atoms. The other hydrogen atom (H1WA) of the water molecule and the two hydrogen atoms of the carbon atoms (C6 and C16) were left to refine freely. A final difference Fourier map showed no residual density outside: 0.310 and −0.261e.Å^{-3}. CCDC No. 795727 contains the supplementary

Table 1
Crystal data and structure refinement for [VO(acac)(pydx-aepy)]·H_2O **(1)**[a].

Formula	$C_{20}H_{25}N_3O_6V$
M_r	454.37
T [K]	153.2
λ, Å [Mo, K_α]	0.71073
Crystal system	Monoclinic
Space group	$P\bar{1}$
a [Å]	6.8719(11)
b [Å]	13.305(2)
c [Å]	13.325(2)
α [°]	118.381(8)
β [°]	91.570(8)
γ [°]	97.907(8)
Z	2
Volume [Å^3]	1055.7(3)
ρ_{calcd} [gcm^{-3}]	1.429
μ mm^{-1}	0.511
Reflections measured	19025
Independent reflections[b]	2894
R (int)	0.0392
Goodness-of-fit on F^2	1.079
R_1 [c]	0.0401
wR_2 (all data)[c]	0.1056

[a] The structure was solved using SHELXS Program for Crystal Structure Determination and refined with SHELXL Program for Crystal Structure Refinement.
[b] $I > 2\sigma(I)$.
[c] $R_1 = \Sigma||F_0| - |F_c||/\Sigma|F_0|$, $wR_2 = \{\Sigma[w(|F_0|^2 - |F_c|^2|)^2]/\Sigma[w(F_0^4)]\}^{1/2}$.

crystallographic data for this paper. This data can be obtained free of charge from the Cambridge Crystallographic Data Centre via www.ccdc.cam.ac.uk/data_request/cif. Crystal data and details of the data collection and refinement for the new complex is collected in Table 1.

2.4. Catalytic activity studies

We have used [V^VO_2(pydx-aepy)]-Y as catalyst to carry out the oxidation of styrene, methyl phenyl sulfide, diphenyl sulfide and cyclohexene. All reactions were carried out in a 50 ml two-necked reaction flask fitted with a water condenser.

2.4.1. Oxidation of styrene

In a typical reaction, styrene (0.52 g, 5 mmol) and aqueous 30% H_2O_2 (1.14 g, 10 mmol) were taken in 5 ml of acetonitrile and temperature of the reaction mixture was raised to 80 °C. The catalyst, [V^VO_2(pydx-aepy)]-Y (0.0125 g) was added to the above reaction mixture and stirred. Oxidised products were analysed quantitatively by gas chromatography during the reaction by withdrawing small aliquots of the reaction mixture at every 30 min intervals. The identities of the products were confirmed by GC–MS. The effects of various parameters, such as amounts of oxidant, catalyst and solvent as well as temperature of the reaction medium were studied in order to see their effect on the conversion and selectivity of the reaction products.

2.4.2. Oxidation of methyl phenyl sulfide and diphenyl sulfide

Methyl phenyl sulfide (1.24 g, 10 mmol) or diphenyl sulfide (1.86 g, 10 mmol), 30% aqueous H_2O_2 (1.14 g, 10 mmol) and catalyst (0.020 g) in acetonitrile were stirred at room temperature and the reaction was monitored by withdrawing samples at different time intervals and analysing them quantitatively by gas chromatography. The identities of the products were confirmed as mentioned above.

2.4.3. Oxidation of cyclohexene

Cyclohexene (0.82 g, 10 mmol), aqueous 30% H_2O_2 (2.27 g 20 mmol) and catalyst (0.010 g) were mixed in acetonitrile (10 ml), and the reaction mixture was heated at 80 °C with continuous stirring. The reaction products were analyzed and identified as mentioned above.

3. Results and discussion

3.1. Synthesis and solid state characteristics

Reaction between equimolar amounts of [$V^{IV}O(acac)_2$] and the ligand Hpydx-aepy (**I**) in dry, refluxing methanol yields the brown oxidovanadium(IV) complex [$V^{IV}O$(acac)(pydx-aepy)] **(1)**. The ligand coordinates out of its monoanionic (ONN(1-)) form; Eq. (1):

$$[V^{IV}O(acac)_2] + \text{Hpydx-aepy} \rightarrow [V^{IV}O(acac)(\text{pydx-aepy})] + \text{Hacac} \quad (1)$$

Complex 1 exhibits a magnetic moment of 1.72 μ_B at ambient temperature; the normal spin only value for a d^1 system being 1.73 μ_B. The addition of H_2O_2 to **1** yields the oxidoperoxido vanadium(V) complex **2**, as shown by Eq. (2). Aerial oxidation of [$V^{IV}O$(acac)(pydx-aepy)] in solution ended up with diamagnetic vanadium(V) species but this could not be isolated in the solid state:

$$2[V^{IV}O(acac)(\text{pydx-aepy})] + 3H_2O_2 \rightarrow 2[V^{V}O(O_2)(\text{pydx-aepy})] + 2\text{Hacac} + 2H_2O \quad (2)$$

Synthesis of dioxidovanadium(V) complex encapsulated in the nano-cavity of zeolite-Y involves two steps: (i) the exchange of $V^{IV}O$ with Na-Y in aqueous solution and (ii) the reaction of vanadium exchanged zeolite i.e. [$V^{IV}O$]-Y **(3)** with excess Hpydx-aepy in methanol where ligand slowly enters into the cavity of zeolite-Y due to its flexible nature and interacts with metal ions to give possibly oxidovanadium(IV) complex loaded zeolite-Y. Extraction of impure samples with methanol using Soxhlet extractor removed excess free ligand and stirring in DMF removed neat metal complex formed on the surface of the zeolite, if any. The initially formed oxidovanadium(IV) species slowly oxidises by air in solution to give dioxidovanadium(V) complex [V^VO_2(pydx-aepy)]-Y **(4)**. The remaining uncomplexed metal ions in zeolite were removed by exchanging with aqueous 0.01 M NaCl solution. As impure sample was extracted well, the vanadium (2.6%) and nitrogen (2.2%) contents found after encapsulation is only due to the presence of dioxidovanadium(V) complex in the cavities of the zeolite-Y. As pyridoxal containing dioxidovanadium(V) complex may have tendency to stabilize as polynuclear species e.g. complex [$K(H_2O)_2$][V^VO_2(pydx-inh)] [29], the encapsulation of dioxidovanadium(V) complex [V^VO_2(pydx-aepy)] in the cavity of zeolite-Y presents an example of stabilisation of monomeric dioxidovanadium(V) complex of this type. Scheme 2 provides structures of the complexes described here and characterized on the basis of spectroscopic (IR, UV/vis and ^{51}V NMR) data, elemental analyses, FE-SEM, X-ray powder diffraction patterns and single crystal X-ray diffraction analysis of complex **1**.

3.2. Structure description of [$V^{IV}O$(acac)(pydx-aepy)]·H_2O (**1**)

The molecular structure of [$V^{IV}O$(acac)(pydx-aepy)]·H_2O **(1)** together with the atom-numbering scheme is shown in Fig. 1; Table 2 provides selected bond lengths and bond angles. In complex **1**, the V^{IV} centre is six-coordinated with an octahedral geometry. The ONN monobasic tridentate ligand, terminal oxygen atom (O3) and two oxygen atoms of the acac group complete the coordination sphere. The presence of acac ions obstructs the formation of dinuclear species [30]. The V1–O3 bond has typical V=O distance of

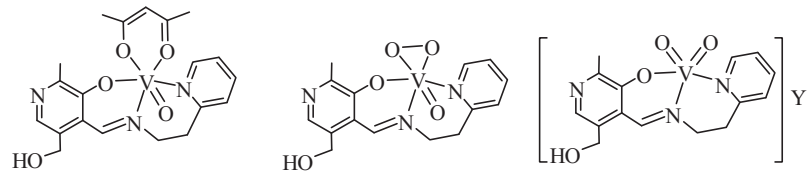

[$V^{IV}O$(acac)(pydx-aepy)] (**1**) [$V^{V}O(O_2)$(pydx-aepy)] (**2**) [$V^{V}O_2$(pydx-aepy)]-Y (**4**)

Scheme 2. Structures of complexes prepared in this paper. Y represents zeolite-Y frame work.

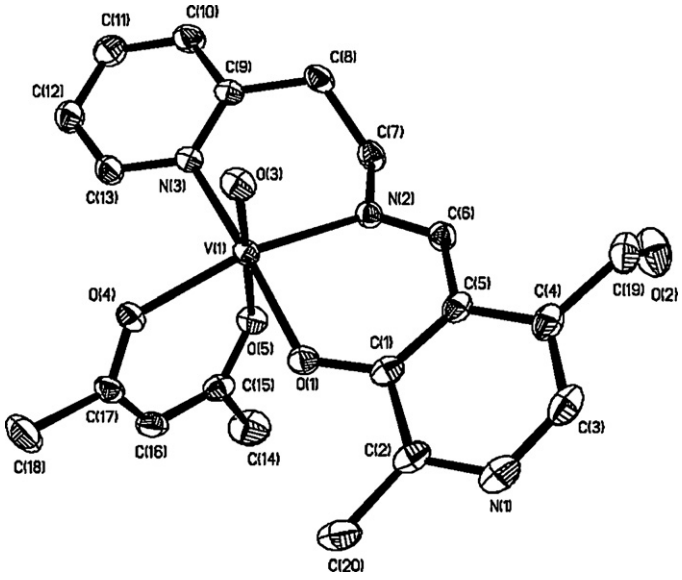

Fig. 1. ORTEP plot (at 30% probability level) of [$V^{IV}O$(acac)(pydx-aepy)] (**1**).

1.599(2) Å. The V1–O4 and V1–O5 distances [V1–O4, 1.9897(19) Å and V1–O5, 2.159(2) Å] are similar to those reported for other V(V)-acac compounds [11,12,14]. The remaining three coordination sites are occupied by the phenolate O atom [V1–O1, 1.9457(19) Å], imine N atom [V1–N2, 2.077(2) Å] and pyridine N atom [V1–N3, 2.193(2) Å]. Again, these bond lengths are similar to other compounds with similar groups bonding to V(IV) centre [11,12,14]. Hydrogen bonds data and symmetry operations are presented in Table 3.

Table 2
Selected bond lengths [Å] and angles [°] for the complex [VO(acac)(pydx-aepy)]·H_2O (**1**).

Lengths (Å)			
V(1)–O(1)	1.9457(19)	V(1)–N(3)	2.193(2)
V(1)–O(3)	1.599(2)	C(1)–O(1)	1.302(3)
V(1)–O(4)	1.9897(19)	N(2)–C(6)	1.277(4)
V(1)–O(5)	2.159(2)	N(2)–C(7)	1.466(3)
V(1)–N(2)	2.077(2)		
Angles (°)			
O(3)–V(1)–O(1)	103.48(10)	O(1)–V(1)–N(3)	164.73(9)
O(3)–V(1)–O(4)	98.61(9)	O(4)–V(1)–N(3)	92.05(8)
O(1)–V(1)–O(4)	86.55(8)	N(2)–V(1)–N(3)	91.02(9)
O(3)–V(1)–N(2)	96.17(10)	O(5)–V(1)–N(3)	80.34(8)
O(1)–V(1)–N(2)	86.58(9)	C(1)–O(1)–V(1)	128.74(17)
O(4)–V(1)–N(2)	164.80(9)	C(6)–N(2)–C(7)	117.5(2)
O(3)–V(1)–O(5)	171.91(9)	C(6)–N(2)–V(1)	124.42(19)
O(1)–V(1)–O(5)	84.40(8)	C(7)–N(2)–V(1)	117.81(18)
O(4)–V(1)–O(5)	83.53(8)	C(13)–N(3)–C(9)	117.8(2)
N(2)–V(1)–O(5)	82.32(8)	C(13)–N(3)–V(1)	118.03(18)
O(3)–V(1)–N(3)	91.77(9)	C(9)–N(3)–V(1)	123.99(19)

3.3. IR spectral studies

Table 4 presents IR spectral data of compounds. IR spectrum of complex, [$V^{IV}O$(acac)(pydx-aepy)] exhibits a sharp band at 943 cm^{-1} which is characteristic of ν(V=O) stretch. The peroxide complex [$V^{V}O(O_2)$(pydx–aepy)] is poor stable and looses oxygen at room temperature. However, the freshly prepared complex exhibits three IR active vibrational modes associated with the peroxido moiety $\{V(O_2)^{3+}\}$ at 830, 756 and 590 cm^{-1}, and are assigned to the O–O intra-stretch (ν_1), the antisymmetric $V(O_2)$ stretch (ν_3), and the symmetric $V(O_2)$ stretch (ν_2), respectively. The presence of these bands confirms the common η^2-coordination of the peroxido group. In addition, a sharp band appearing at 934 cm^{-1} is assigned to the ν(V=O) stretch. These peaks agree well with those reported for several [$V^{V}O(O_2)$L] complexes [31]. Location of bands due to *cis*-VO_2 structure in zeolite-Y encapsulated vanadium complex has not been possible due to appearance of a strong and broad band at ca. 1000 cm^{-1} due to zeolite frame work. The ligand Hpydx-aepy was not isolable in the solid state, however, its in situ prepared methanolic solution exhibited two sharp bands at 1631 and 1595 cm^{-1} due to the ν(C=N) of the azomethine and ring stretch, respectively. The band due to azometnine nitrogen normally shifts towards lower wavenumber while that of ring nitrogen moves towards higher side. All the complexes also exhibit one or two sharp bands in the 1600–1637 cm^{-1}, indicating the coordination of the azomethine/ring nitrogen to the vanadium. The presence of multiple bands of medium intensity covering 2800–2900 cm^{-1} regions is consistent with the presence of $-CH_2$ groups.

3.4. Field-emission-scanning electron micrograph (FE-SEM) and energy dispersive X-ray analysis (EDX) studies

The field emission scanning electron micrograph (FE-SEM) of [$V^{V}O_2$(pydx-aepy)]-Y along with their energy dispersive X-ray analysis (EDX) profile are presented in Fig. 2. Accurate information

Table 3
Hydrogen bonds data and symmetry operations.

D–H	H···A	D···A	<(DHA)	
0.94	1.93	2.774(4)	148.5	O(2)–H(2O)···O(1W)
1.02	1.85	2.830(4)	161.2	O(1W)–H(1WB)···O(2)_$1
0.77(4)	2.03(5)	2.780(4)	165(5)	O(1W)–H(1WA)···N(1)_$2

Symmetry transformations used to generate equivalent atoms:
$1 [−x, −y−1, −z].
$2 [x − 1, y, z].

Table 4
IR spectral data (cm^{-1}) of complexes.

Compound	ν(C=N)	ν(V=O)
Hpydx-aepy (**I**)	1631, 1595	
[$V^{IV}O$(acac)(pydx-aepy)] (**1**)	1634, 1600	943
[$V^{V}O(O_2)$(pydx-aepy)] (**2**)[a]	1637, 1618	934
[$V^{V}O_2$(pydx-aepy)]-Y (**4**)	1635	–

[a] Bands due to the peroxido group at 830, 756 and 590 cm^{-1}.

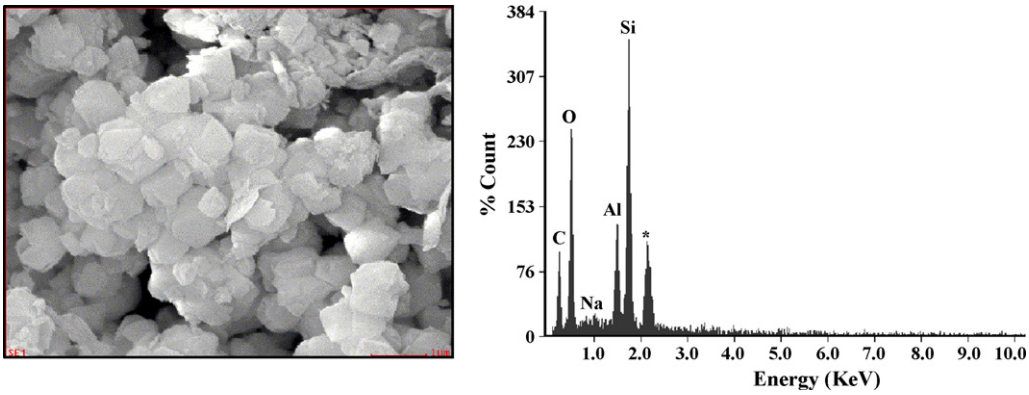

Fig. 2. Scanning electron micrograph (left) and energy dispersive X-ray analysis (EDX) profile (right) of [$V^{V}O_2$(pydx-aepy)]-Y. Asterisk in EDX shows signal for gold.

on the morphological changes in terms of exact orientation of ligand coordinated to the metal ion has not been possible due to poor loading of the metal complex. However, it is clear from the micrograph that zeolite having encapsulated vanadium complex has well defined crystals and there is no indication of the presence of any metal ion or complex on the surface. Energy dispersive X-ray analysis plot, evaluated semi-quantitatively, supports this conclusion as no vanadium or nitrogen contents were noted on the spotted surface in the plot for [$V^{V}O_2$(pydx-aepy)]-Y. Only small amount of carbon (ca. 9.6%) but no nitrogen on the spotted surfaces suggest the presence of trace amount of adsorbed solvent (methanol) from which it was finally washed after Soxhlet extraction. An amount of ca. 2.6% sodium suggests the exchange of remaining free vanadium ion by sodium ion during re-exchange process. The average silicon and aluminum percentage obtained were ca. 38.5% and ca. 12.2%, respectively.

3.5. Powder X-ray diffraction studies

The powder X-ray diffraction patterns of Na-Y, [V^{IV}O]-Y and encapsulated complex [$V^{V}O_2$(pydx-aepy)]-Y were recorded at 2θ values between 5 and 70°, and patterns are presented in Fig. 3. Essentially similar diffraction patterns in encapsulated complex, [V^{IV}O]-Y and Na-Y were noticed except a slightly weaker intensity for the encapsulated complex. These observations indicate that the framework of the zeolite has not undergone any structural change during incorporation of the complex i.e. crystallinity of the zeolite-Y is preserved during encapsulation. No new peaks due to encapsulated complex were detected in the zeolite encapsulated sample possibly due to very low percentage loading of metal complex.

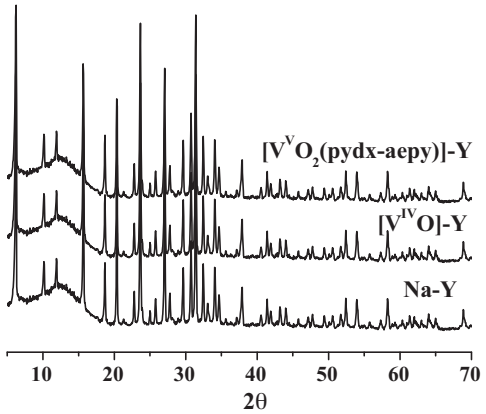

Fig. 3. XRD patterns of Na-Y, [V^{IV}O]-Y and [$V^{V}O_2$(pydx-aepy)]-Y.

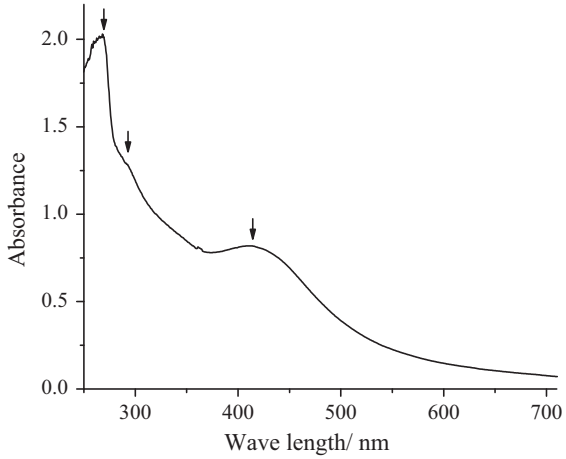

Fig. 4. Electronic spectrum of [$V^{V}O_2$(pydx-aepy)]-Y **(5)** recorded after dispersing in Nujol.

3.6. Electronic absorption spectra

The electronic spectral profile of encapsulated complex is presented in Fig. 4 and the corresponding data along with other compounds are presented in Table 5. The electronic spectrum of [$V^{V}O_2$(pydx-aepy)]-Y **(4)** exhibits a lmct band at 410 nm along with two UV bands compatible with dioxidovanadium(V) species in the super cages of the cavity of the zeolite-Y. Other complexes exhibit lmct band at ca. 400 nm along with four UV bands. The lower energy (less intense) bands appearing at 535 and 768 nm in [VO(acac)(pydx-aepy)] **(1)** are assigned due to d–d transitions. As complex **4** has $3d^0$ configuration, d → d bands are not expected.

3.7. ^{51}V NMR spectrum

The ^{51}V NMR spectrum of [$V^{V}O(O_2)$(pydx-aepy)] could only be recorded with the freshly prepared complex in DMSO-d_6. The resonance was broadened as a consequence of the quadrupolar interaction (^{51}V: nuclear spin = 7/2, quadrupole moment = −4.8 fm); line widths at half height were approximately 200 Hz, which is still considered narrow in ^{51}V NMR spectroscopy

Table 5
Electronic spectral data of complexes.

Compounds	Solvent	λ_{max} (nm)
[$V^{IV}O$(acac)(pydx-aepy)] **(1)**	MeOH	225, 258, 305, 395, 535, 768
[$V^{V}O(O_2)$(pydx-aepy)] **(2)**	MeOH	225, 258, 337, 435
[$V^{V}O_2$(pydx-aepy)]-Y **(4)**	Nujol	267, 293, 410

[32,33]. The complex did not show clean ^{51}V NMR signal due to its poor stability. In fact, it exhibits two sharp peaks at −497 (minor) and −519 ppm (major) which seems to be due to [$V^{V}O_2$(pydx-aepy)(DMSO)] and [$V^{V}O_2$(pydx-aepy)]. This is based on the recently reported very similar complex e.g. [$V^{V}O_2$(sal-aepy)] that exhibits two resonances at −491 and −517 ppm in DMSO-d_6 [12] All these results affirm the poor stability of peroxide species and its conversion into a mixture of vanadium(V) complexes in DMSO. However, addition of one drop of 30% aqueous H_2O_2 to the above solution gives rise to an additional weak signal at −575 ppm along with the reduction of the intensity of originally appeared two resonances and this is indicative of the formation of peroxide species at the expense of the two species existed in solution [12].

3.8. Reactivity of [$V^{IV}O$(acac)(pydx-aepy)] (**1**) with H_2O_2

Treatment of complex [$V^{IV}O$(acac)(pydx-aepy)] with H_2O_2 at ca 10 °C yielded poor stable oxidoperoxidovanadium(V) complex [$V^{V}O(O_2)$(pydx-aepy)], the generation of which in solution has also been established by electron absorption spectroscopy. Changes in the absorption spectra during titration of the methanolic solution of [$V^{IV}O$(acac)(pydx-aepy)] with aqueous 30% H_2O_2 dissolved in methanol are shown in Fig. 5. The d–d bands appearing at 535 and 768 nm slowly disappeared (Fig. 5a and in set there in). The charge transfer band appearing at 395 nm shifted to 435 nm along with decrease in intensity while band due to n–π* transition at 305 nm shifted to 337 nm with decrease in intensity. With increase in the maxima, bands at 225 and 258 nm remained nearly constant (Fig. 5b). The features of the final spectrum is similar to that of the isolated peroxido complex [$V^{V}O(O_2)$(pydx-aepy)].

3.9. Catalytic activity studies

3.9.1. Oxidation of styrene

Oxidation of styrene, catalysed by [$V^{V}O_2$(pydx-aepy)]-Y using aqueous 30% H_2O_2 as oxidant gave four oxidation products namely, styrene oxide, benzaldehyde, 1-phenylethane-1,2-diol and benzoic acid along with small amount of unidentified product (Scheme 3). Hulea and Dumitriu [34] have reported some of these product during the oxidation of styrene using TS-1 and MCM-41. At least five oxidation products have been obtained using polymer-anchored catalysts PS-[$V^{IV}O$(sal-ohyba)·DMF] [35] and PS-K[$V^{V}O(O_2)$(L)] [L = 2-(2-pyridyl)benzimidazole and 2-(3-pyridyl)benzimidazole] [36].

The reaction conditions were optimised for the maximum oxidation of styrene by studying four different parameters viz. the effect of amount of oxidant (moles of H_2O_2 per mole of styrene),

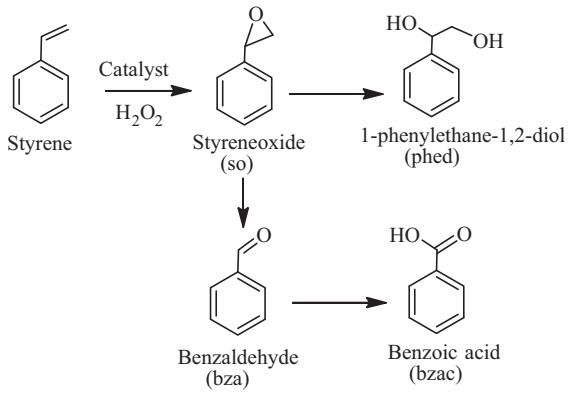

Scheme 3. Oxidation of styrene with H_2O_2 catalysed by [$V^{V}O_2$(pydx-aepy)]-Y.

catalyst (amount of catalyst per mole of styrene), temperature and solvent amount of the reaction mixture in detail.

The effect of oxidant was studied considering styrene: aqueous 30% H_2O_2 molar ratios of 1:1, 1:2, and 1:3 where the mixture of styrene (0.52 g, 5 mmol), catalyst (0.0125 g) and oxidant were taken in 5 ml of CH_3CN and the reaction was carried out at 80 °C. As illustrated in see Fig. S1 (supporting information) and presented in entry nos. 1, 2 and 3 of Table 6, the percent conversion of styrene improved from 79.7% to 94.0% on increasing the styrene: oxidant ratio from 1:1 to 1:2. Further increasing this ratio to 1:3, though affected the conversion but not very significantly (96.6%), suggesting that 1:2 (styrene:H_2O_2) molar ratio is sufficient enough to perform the reaction with good conversion.

Similarly, for three different amounts viz. 0.010, 0.0125 and 0.015 g of catalyst and styrene to H_2O_2 molar ratio of 1:2 under above reaction conditions, 0.010 g catalyst gave only 54.1% conversion while 0.0125 and 0.015 g catalyst produced 94.0% and 97.6% conversions, respectively (Fig. S2 and entry nos. 2, 4 and 5 of Table 6). However, at the expense of H_2O_2, 0.0125 g catalyst can be considered sufficient enough to carry out the reaction. Further, the turn over rates (TOF h^{-1} = moles of substrate converted per mole of catalyst per hour) is also higher for 0.0125 g catalyst (TOF = 105.4) to achieve 94.0% conversion of styrene.

Temperature of the reaction mixture has also influenced on the performance of the catalyst. Amongst three different temperatures of 60, 70 and 80 °C for the fixed operating condition of styrene (0.52 g, 5 mmol), H_2O_2 (1.14 g, 10 mmol), [$V^{V}O_2$(pydx-aepy)]-Y (0.0125 g) and MeCN (5 ml), running the reaction at 80 °C gave much better conversion (Fig. S3 and entry nos. 2, 6 and 7 of Table 6). More over, time required in achieving the maximum conversion was also reduced on carrying out the reaction at 80 °C.

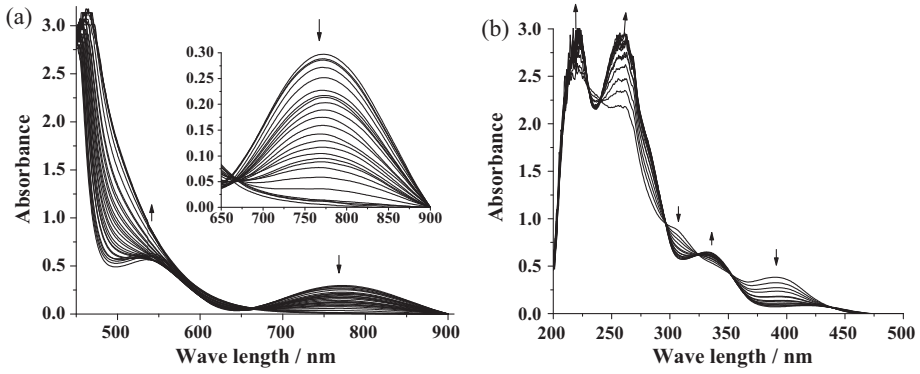

Fig. 5. UV–vis spectral changes observed during titration of [$V^{IV}O$(acac)(pydx-aepy)] with H_2O_2. (a) The spectra were recorded after successive additions of one drop portions of H_2O_2 (ca. 12 mmol of 30% H_2O_2 dissolved in 10 ml of methanol) to 50 ml of ca. 10^{-3} M solution of [$V^{IV}O$(acac)(pydx-aepy)] in methanol at every 5 min interval. (b) The equivalent titration, but with lower concentrations of a [$V^{IV}O$(acac)(pydx-aepy)] solution (ca. 10^{-4} M).

Table 6
Conversion of styrene (0.52 g, 5 mmol) using [$V^{V}O_2$(pydx-aepy)]-Y as catalyst in 7 h of reaction time under different reaction conditions.

Entry no.	Catalyst (g)	Temp. (°C)	H_2O_2 (g, mmol)	CH_3CN (ml)	Conversion %
1	0.0125	80	0.57, 5	5	79.7
2	0.0125	80	1.14, 10	5	94.0
3	0.0125	80	1.71, 15	5	96.6
4	0.010	80	1.14, 10	5	54.1
5	0.015	80	1.14, 10	5	97.6
6	0.0125	60	1.14, 10	5	54.8
7	0.0125	70	1.14, 10	5	77.0
8	0.0125	80	1.14, 10	2	87.7
9	0.0125	80	1.14, 10	7.5	54.9

Variation in the volume of the solvent was also studied by taking 2, 5 and 7.5 ml of CH_3CN (Table 6). It was observed that 5 ml of CH_3CN was sufficient enough for styrene (0.52 g, 5 mmol), H_2O_2 (1.14 g, 10 mmol) and [$V^{V}O_2$(pydx-aepy)]-Y (0.0125 g) to get good transformation of styrene while running the reaction at 80 °C. Thus, all reaction conditions as concluded above were considered essential and applied for the maximum transformation of styrene into a mixture of oxidation products.

The conversion of styrene and the selectivity of different reaction products using [$V^{V}O_2$(pydx-aepy)]-Y as catalyst under the optimised reaction conditions (entry no. 2 of Table 6) have been analysed as a function of time and are presented in Fig. 6. It is clear from the plot that a selectivity of 80.7% of benzaldehyde has been obtained at a conversion of 22.8% of styrene in 1 h of the reaction time. This selectivity decreases slowly with time and reaches to 58.3% with the increase of the conversion of styrene to 94.0% in 7 h. Starting with 6.9% in first hour, the selectivity of 1-phenylethane-1,2-diol increases considerably with the conversion of styrene and reaches to 29.6%. The selectivity of other two products styrene oxide and benzoic acid is poor in the beginning but the former one slowly decreases while later one increases. However, their overall formations are not much even after 7 h of the reaction time. After 7 h only minor changes have been observed in the selectivity of the different reaction products.

Under optimised reaction conditions, the selectivity of the different oxidation products formed varies in the order: benzaldehyde (58.3%) > 1-phenylethane-1,2-diol (29.6%) > benzoic acid (6.6%) > styrene oxide (4.3%). The formation of benzaldehyde in highest yield may be due to the nucleophilic attack of H_2O_2 on the styrene oxide formed in the first step, followed by the cleavage of the intermediate hydroperoxy styrene. Benzaldehyde formation may also be facilitated by direct oxidative cleavage of the styrene side chain double bond via a radical mechanism [34]. The formation of 1-phenylethane-1,2-diol formation is possible through hydrolysis of styrene oxide by water present in H_2O_2.

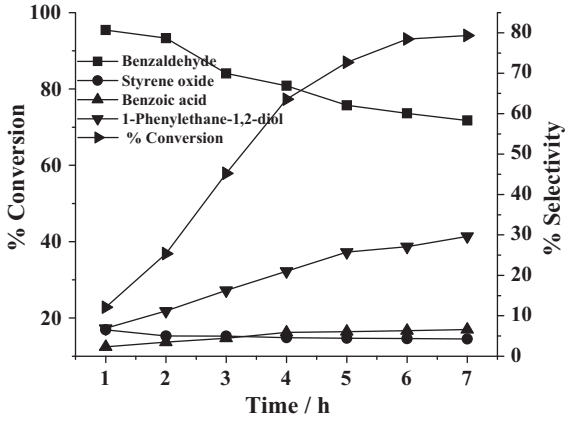

Fig. 6. Conversion of styrene and variation in the selectivity of different reaction products as a function of time using [$V^{V}O_2$(pydx-aepy)]-Y as catalyst.

Complex [$V^{IV}O$(acac)(pydx-aepy)] has been used as a catalyst precursor to compare its catalytic activity with encapsulated complex. Interestingly, this exhibited 85.9% conversion when complex (0.0028 g, 0.007 mmol), styrene (0.52 g, 5 mmol) and 30% H_2O_2 (1.14 g, 10 mmol) were taken in 5 ml of acetonitrile and the reaction was carried out at 80 °C. Here, the selectivity of different products follow the order: benzaldehyde (60.5%) > 1-phenylethane-1,2-diol (24.4%) > benzoic acid (10.9%) > styrene oxide (3.2%). Thus, the order is same as obtained by encapsulated complex but the selectivity of individual products differs in two cases. Blank reaction under above reaction conditions gave 3% conversion. Thus, neat as well as encapsulated complexes both are good in catalytic activity. However, the recyclable nature and no leaching of [$V^{V}O_2$(pydx-aepy)]-Y makes it better over neat one.

.

3.9.2. Oxidation of methyl phenyl sulfide and diphenyl sulfide

It is known that vanadium dependent haloperoxidases [5,37] and model complexes catalyse the oxidation, by H_2O_2, of sulfides (thioethers) to sulfoxides and further to sulfones [38,39]. We have tested the catalytic potential of [$V^{V}O_2$(pydx-aepy)]-Y to mimic the sulfoxidation considering methyl phenyl sulfide and diphenyl sul-

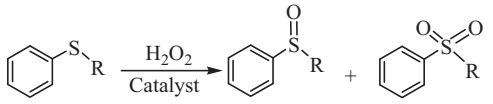

R = CH_3: Methyl phenyl sulfide
R = C_6H_5: Diphenyl sulfide

Scheme 4.

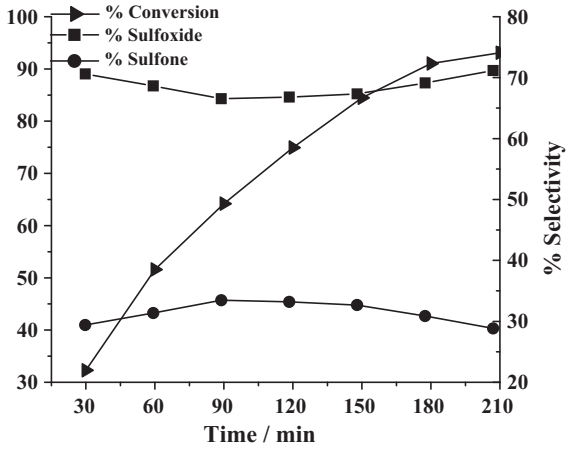

Fig. 7. Plots showing percentage selectivity of methyl phenyl sulfoxide and methyl phenyl sulfone formation, and percentage conversion of methyl phenyl sulfide as a function of time. Reaction condition: methyl phenyl sulfide (1.24 g, 10 mmol), H_2O_2 (2.27 g, 20 mmol), [$V^{V}O_2$(pydx-aepy)]-Y (0.020 g) and CH_3CN (5 ml).

Table 7
Conversion of methyl phenyl sulfide (1.24 g, 10 mmol) or diphenyl sulfide (1.86, 10 mmol) using $[V^{V}O_2(pydx\text{-}aepy)]$-Y as catalyst in 7 h of reaction time under different reaction conditions.

Entry No.	Catalyst (g)	Substrate[a]	H_2O_2 (g, mmol)	CH_3CN (ml)	Conversion %
1	0.020	mps	1.14, 10	5	82.9
2	0.020	mps	1.70, 15	5	87.9
3	0.020	mps	2.27, 20	5	93.1
4	0.020	mps	3.41, 30	5	96.9
5	0.025	mps	2.27, 20	5	95.0
6	0.030	mps	2.27, 20	5	75.4
7	0.035	mps	2.27, 20	5	68.4
8	0.015	dps	1.14, 10	10	48.9
9	0.015	dps	2.27, 20	10	27.0
10	0.015	dps	3.41, 30	10	23.7
11	0.010	pds	1.14, 10	10	35.9
12	0.020	dps	1.14, 10	10	63.0
13	0.025	dps	1.14, 10	10	63.6
14	0.020	dps	1.14, 10	5	63.6
15	0.020	dps	1.14, 10	15	67.0

[a] mps: methyl phenyl sulfide and dps: diphenyl sulfide.

fide. The oxidation of these sulfides gave a mixture of two products; Scheme 4

The reaction conditions were optimised for the maximum oxidation of methyl phenyl sulfide by studying three different parameters viz. the effect of amount of oxidant (moles of H_2O_2 per mole of methyl phenyl sulfide) and catalyst (amount of catalyst per mole of methyl phenyl sulfide) and solvent of the reaction mixture in detail.

The effect of oxidant was studied by considering substrate to oxidant ratios of 1:1, 1:1.5, 1:2 and 1:3 for the fixed amount of $[V^{V}O_2(pydx\text{-}aepy)]$-Y (0.020 g) and methyl phenyl sulfide (1.24 g, 10 mmol) in 5 ml of acetonitrile and reaction was monitored at room temperature. As shown in Fig. S4 and presented in entry nos. 1–4 of Table 7, the oxidation of methyl phenyl sulfide dependents upon the amount of oxidant (30% aqueous H_2O_2) used in the reaction. At a H_2O_2:methyl phenyl sulfide molar ratio of 1:1, a maximum of 82.9% conversion was achieved in ca. 3.5 h. This conversion goes on increasing on further increasing this ratio. At lowest H_2O_2:methyl phenyl sulfide concentration of 1:1, the selectivity for the formation of methyl phenyl sufoxide was highest (74.2%) and this takes up decreasing trend on increasing this ratio i.e. 73.1% at 1:1.5, 71.2% at 1:2 and 63.4% at 1:3 ratio. However, H_2O_2:methyl phenyl sulfide molar ratio of 1:2 with methyl phenyl sulfide conversion of 93.1% and TOF of 261 seems to be the best one as increasing this ratio to 1:3 increases TOF only marginally while decreases the formation of sulfoxide sharply.

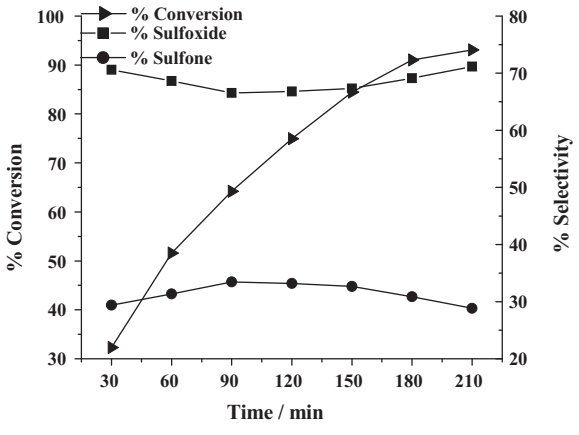

Fig. 8. Plots showing percentage selectivity of diphenyl sulfoxide and diphenyl sulfone formation and percentage conversion of diphenyl sulfide as a function of time. Reaction condition: diphenyl sulfide (1.86 g, 10 mmol), H_2O_2 (1.14 g, 10 mmol), $[V^{V}O_2(pydx\text{-}aep)]$-Y (0.020 g) and acetonitrile (15 ml).

Similarly, four different amounts of $[V^{V}O_2(pydx\text{-}aepy)]$-Y viz. 0.020, 0.025, 0.030, 0.035 g were taken under the above optimised reaction conditions i.e. methyl phenyl sulfide (1.24 g, 10 mmol), 30% H_2O_2 (2.27 g, 20 mmol) and CH_3CN (5 ml) to see the effect of amount of catalyst on the reaction and results are shown in Fig. S5 and presented in entry nos. 1 and 5–7 of Table 7. It was observed that increasing the amount of catalyst from 0.020 g to 0.025 g improved the conversion from 93.1% to 95.0% but further increment of catalyst resulted in the lower conversion. As TOF value for 0.020 g (TOF = 260.8 h^{-1}) catalyst is higher than for 0.025 g (TOF = 213 h^{-1}), while conversion difference for these amounts is not much (ca. 4%), an amount of 0.020 g catalyst was considered to be optimum for best result. The amount of solvent also has influence on the oxidation of methyl phenyl sulfide. It was concluded that 5 ml CH_3CN was sufficient enough to effect maximum conversion under above optimised reaction conditions.

Therefore, from these experiments, the best reaction conditions for the maximum oxidation of methyl phenyl sulfide are: substrate (1.24 g, 10 mmol), H_2O_2 (2.27 g, 20 mmol), $[V^{V}O_2(pydx\text{-}aepy)]$-Y (0.020 g) and CH_3CN (5 ml). The percent conversion of methyl phenyl sulfide under the optimised reaction conditions and the selectivity of reaction products as a function of time are shown in Fig. 7. It is clear from the plot that both the products started to form with the conversion of methyl phenyl sulfide. However, their selectivity (70.6% for methyl phenyl sulfoxide and 29.2% for methyl phenyl sulfone) after 1 h remained nearly constant while conversion increased from 32.3 to 93.1% in 3.5 h.

Using $[V^{IV}O(acac)(pydx\text{-}aepy)]$ as catalyst precursor and considering its same mole concentration as of $[V^{V}O_2(pydx\text{-}aepy)]$-Y under above reaction conditions (i.e. $[V^{IV}O(acac)(pydx\text{-}aepy)]$ (0.0045 g, 0.01 mmol), methyl phenyl sulfide (1.24 g, 10 mmol), 30% H_2O_2 (2.27 g, 20 mmol) and acetonitrile (5 ml)), a maximum of 96.3% conversion of methyl phenyl sulfide was achieved. Here selectivity of sulfoxide and sulfone were 65% and 35%, respectively.

The catalytic action of $[V^{V}O_2(pydx\text{-}aepy)]$-Y towards the oxidation of diphenyl sulfide was found to be different from methyl phenyl sulfide. Here, at a diphenyl sulfide to oxidant molar ratio of 1:1 for the fixed amount of diphenyl sulfide (1.86 g, 10 mmol), $[V^{V}O_2(pydx\text{-}aepy)]$-Y (0.015 g) and CH_3CN (10 ml), reac-

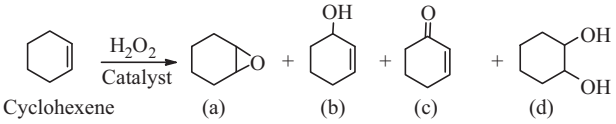

Scheme 5. (a) Cyclohexeneoxide, (b) 2-cyclohexene-1-ol, (c) 2-cyclohexene-1-one and (d) cyclohexane-1,2-diol.

Table 8
Conversion of cyclohexene (0.82 g, 10 mmol) using $[V^{V}O_2(pydx\text{-}2aep)]$-Y as catalyst in 6 h of reaction time under different reaction conditions.

Entry No.	Catalyst (g)	Temp. (°C)	H_2O_2 (g, mmol)	CH_3CN (ml)	Conversion %
1	0.010	80	1.14, 10	10	85.0
2	0.010	80	2.27, 20	10	94.1
3	0.010	80	3.41, 30	10	96.0
4	0.005	80	2.27, 20	10	75.8
5	0.015	80	2.27, 20	10	97.4
6	0.010	80	2.27, 20	2	98.5
7	0.010	80	2.27, 20	5	96.1
8	0.010	60	2.27, 20	5	72.0
9	0.010	70	2.27, 20	5	87.5
10[a]	0.010	80	2.27, 20	5	93.7
11[b]	0.010	80	2.27, 20	5	93.1

[a] First recycle of used catalyst.
[b] Second recycle of used catalyst.

tion required ca. 7 h to acquire equilibrium and only 48.9% dipheyl sulfide was converted into products at room temperature. Increasing this ratio only slightly influenced on the equilibrium towards left but the over all conversion was decreased (Fig. S6 and entry nos. 8–10 of Table 7). The selectivity of the formation of sulfoxide was better (86.0%) at 1:1 ratio while at diphenyl sulfide to oxidant (H_2O_2) molar ratios of 1:2 and 1:3, the selectivity decreased to 71.9 and 66.3%, respectively.

Four different amount of catalyst viz. 0.010, 0.015, 0.020, and 0.025 g were used for the fixed amount of diphenyl sulfide (1.86 g, 10 mmol), H_2O_2 (1.14 g, 10 mmol) and acetonitrile (10 ml) to see the effect of catalyst and obtained results are plotted in Fig. S7 and presented in entry nos. 8 and 11–13 of Table 7 as a function of time. Increasing the amount of catalyst increased the diphenyl sulfide transformation and a maximum of 63.0% conversion was achieved with 0.020 g of catalyst. Further increment of catalyst amount to 0.025 g resulted in only marginal increase (63.6%) in substrate conversion. This has been interpreted in terms of thermodynamic and mass transfer limitations at higher reaction rate. In all cases reaction acquired steady state in ca. 7 h and the selectivity of the formation of diphenyl sulfoxide remained almost constant (ca. 86%).

The influence of the volume of solvent (CH_3CN) on the rate of reaction was also tested and 15 ml of acetonitrile was found to be the best (entry no. 15 of Table 7) under the optimised reaction conditions i.e. diphenyl sulfide (1.86 g, 10 mmol), 30% H_2O_2 (1.14 g, 10 mmol), $[V^{V}O_2(pydx\text{-}aepy)]$-Y (0.020 g) to give a maximum of 67.0% conversion with 66.3% selectivity of diphenyl sulfoxide. However, the selectivity for the diphenyl sulfoxide was 86.0% at 63.6% transformation of diphenyl sulfide in lower amount of solvent (5 ml), We have analysed the conversion of diphenyl sulfide as a function of time considering the best reaction conditions for the maximum oxidation of diphenyl sulfide along with good selectivity towards the formation of diphenyl sulfoxide as concluded above (i.e. diphenyl sulfide (1.86 g, 10 mmol), H_2O_2 (1.14 g, 10 mmol), $[V^{V}O_2(pydx\text{-}aep)]$-Y (0.020 g) and acetonitrile (15 ml)) and results are presented in Fig. 8. About 25% conversion with 92% selectivity of diphenyl sulfoxide was achieved within 1 h. This conversion improved with time and reached to 67% while the selectivity of sulfoxide started going down with time and reached to 66.3% in 7 h, accordingly, the selectivity of diphenyl sulfone reached to 33.8%.

Thus, the catalytic potential of $[V^{V}O_2(pydx\text{-}aepy)]$-Y varies with the sulfide substrates, and different conditions are required to observed effective catalytic activity. In the absence of the catalyst, the reaction mixture gave 35.3% conversion of methyl phenyl sulfide in 10 ml of acetoniitrile with 65.5% selectivity towards sulfoxide, 34.2% towards sulfone and ca. 0.3% an unidentified product. Blank reaction with diphenyl sulfide under the above reaction conditions gave ca. 5% conversion with sulfoxide:sulfone selectivity of 57:43. Thus, catalysts not only improve the conversion of substrates, they alter the selectivity of the products as well.

Considering same mole concentration of neat catalyst precursor, $[V^{IV}O(acac)(pydx\text{-}aepy)]$ under above reaction conditions (i.e. $[V^{IV}O(acac)(pydx\text{-}aepy)]$ (0.0045 g, 0.01 mmol), diphenyl sulfide (1.86 g, 10 mmol) and 30% H_2O_2 (1.14 g, 10 mmol) and acetonitrile (15 ml)), a maximum of 86.1% conversion of diphenyl sulfide was achieved where selectivity of sulfoxide was 83.2%. Thus, neat as well as encapsulated complexes both are good catalysts for the oxidation of organic sulfides. However, the stability and recyclable nature of zeolite-Y encapsulated complex make it better catalyst over neat one.

3.9.3. Oxidation of cyclohexene

Complex $[V^{V}O_2(pydx\text{-}2aep)]$-Y also catalyses the oxidation of cyclohexene by H_2O_2 efficiently to give cyclohexene epoxide, 2-cyclohexene-1-one, 2-cyclohexene-1-ol and cyclohexane-1,2-diol as presented in Scheme 5.

In order to achieve optimum conditions, three different cyclohexene to aqueous 30% H_2O_2 molar ratios viz. 1:1, 1:2 and 1:3 were considered for the fixed amount of cyclohexene (0.82 g, 10 mmol) and catalyst (0.010 g) in 10 ml of MeCN and reaction was carried out at 80 °C. Fig. S8 and entry nos. 1, 2 and 3 of Table 8 presents the results obtained. A maximum of 85.0% conversion was obtained for cyclohexene to H_2O_2 molar ratio of 1:1 in 6 h of reaction time. This conversion reached 94.1% on increasing this ratio to 1:2 while 1:3 ratio has shown only marginal improvement (96.0%) in the conversion.

Under the operating conditions as fixed above i.e. cyclohexene (0.82 g, 10 mmol), 30% H_2O_2 (2.27 g, 20 mmol) in 10 ml of MeCN, the

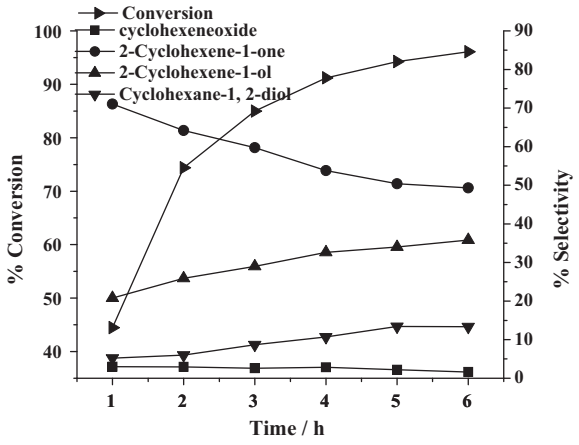

Fig. 9. Plots showing percentage selectivity of cyclohexene oxide, 2-cyclohexene-1-one 2-cyclohexene-1-ol, and cyclohexane-1,2-diol formation and percentage conversion of cyclohexene as a function of time. Reaction condition: cyclohexene (0.82 g, 10 mmol), H_2O_2 (2.27 g, 20 mmol), $[VO_2(pydx\text{-}aepy)]$-Y (0.010 g) acetonitrile (5 ml) and temp. (80 °C).

effect of catalyst considering three different amounts viz. 0.005, 0.010 and 0.015 g as a function of time was studied and results are illustrated in Fig. S9 and presented in entry nos. 2, 4 and 5 of Table 8. It is clear from the plot that 0.010 g catalyst was the best one to obtain a maximum of 94.1% conversion of cyclohexene as 0.015 g catalysts showed only marginal improvement in conversion while 0.005 g catalyst gave much poor result. We have also optimised the amount of solvent (acetonitrile, entry nos. 2, 6 and 7) and temperature (entry nos. 7, 8 and 9) of the reaction and found that 5 ml of solvent and 80 °C reaction temperature were good to obtained 96.1% conversion under above reaction conditions.

The conversion of cyclohexene and selectivity of different reaction products under the optimised reaction conditions (entry no. 7 of Table 8) have been analysed as a function of time and are presented in Fig. 9. It is clear from the plot that at a conversion of 44.5% of cyclohexene in 1 h of reaction time, 3.0% selectivity of cyclohexene epoxide, 71.0% of 2-cyclohexene-1-one, 20.8% of cyclohexene-1-ol and 5.2% of 2-cyclohexe-1,2-diol have been obtained. The selectivity of cyclohexene-1-ol and 2-cyclohexe-1,2-diol increases with time and reaches to 35.8% and 13.4%, respectively, with the increase of the conversion of cyclohexene to 96.1% in 6 h. 2-Cyclohexene-1-one looses its selectivity and reaches to 49.3% while the selectivity of cyclohexene oxide has marginal decreasing trend. After 6 h, only a minor change was noted in the selectivity of the different reaction products. At the end of 6 h, the selectivity of different products follows the order: 2-cyclohexene-1-one (49.3%) > cyclohexene-1-ol (35.8%) > 2-cyclohexane-1,2-diol (13.4%) > cyclohexene epoxide (1.6%). A maximum of 82.4% conversion with neat catalyst precursor [$V^{IV}O$(acac)(pydx-aep)] was obtained under similar conditions where products selectivity varied in the order: 2-cyclohexene-1-one (45.0%) > cyclohexene-1-ol (33.2%) > 2-cyclohexane-1,2-diol (20.2%) > cyclohexene epoxide (1.6%).

3.10. Test for recyclability and heterogeneity of the reaction

The recycle ability of [$V^{V}O_2$(pydx-aepy)]-Y was tested for the oxidation of cyclohexene under similar conditions after separating the used catalyst from the reaction mixture, washing with acetonitrile and drying at ca. 120 °C. First cycle of experiment gave 93.7% while second cycle gave 93.1% conversion of cyclohexene (entry nos. 10 and 11 of Table 8). The products distribution with time and selectivity of the reaction products are nearly preserved as obtained for fresh catalyst within the experimental error. The filtrate collected after separating the solid catalyst were placed into the reaction flasks, and the reaction was continued for all three reactions after adding fresh oxidant for another 2 h. The gas chromatographic analyses showed no further increment in the conversion. This confirms that the reaction did not proceed upon removal of the solid catalyst and hence the catalysis is heterogeneous in nature.

4. Conclusions

We have prepared new complexes, [$V^{IV}O$(acac)(pydx-aepy)] **(1)**, [$V^{V}O(O_2)$(pydx-aepy)] **(2)** with the Schiff base Hpydx-aepy. The crystal and molecular structures of 1 has been determined, confirming the ONN binding mode of the ligand. The formation of poor stable oxidoperoxidovanadium(V) complex [$V^{V}O(O_2)$(pydx-aepy)] **(2)** in solution has also been demonstrated electronic absorption spectroscopically by reacting [$V^{IV}O$(acac)(pydx-aepy)] with aqueous H_2O_2 in methanol The dioxidovanadium(V) complex [VO_2(pydx-aepy)] has been encapsulated in the nano-pores of zeolite-Y and used as catalyst for the oxidation of styrene, methyl phenyl sulfide, diphenyl sulfide and cyclohexene using H_2O_2 and results are very encouraging. The encapsulated catalyst is stable, recyclable and looses its activity only slightly.

Acknowledgements

MRM and MB are thankful to Department of Science and Technology, Government of India, and FA acknowledges Universidade da Coruña for financial support.

Appendix A. Supplementary data

Supplementary data associated with this article can be found, in the online version, at doi:10.1016/j.molcata.2011.04.017.

References

[1] A. Messershmidt, R. Wever, Proc. Natl. Acad. Sci. U.S.A. 93 (1996) 392–396.
[2] M. Weyand, H.J. Hecht, M. Kiess, M.F. Liaud, H. Vilter, D. Schomburg, J. Mol. Biol. 293 (1999) 595–611.
[3] S. Macedo–Ribeiro, W. Hemrika, R. Renirie, R. Wever, A. Messerschmidt, J. Biol. Inorg. Chem. 4 (1999) 209–219.
[4] A. Butler, in: J. Reedijk, E. Bouwman (Eds.), Bioinorganic Catalysis, 2nd ed., Marcel Dekker, New York, 1999 (Chapter 5).
[5] D. Rehder, Bioinorganic Vanadium Chemistry, Wiley & Sons, New York, 2008.
[6] B.J. Hamstra, A.L.P. Houseman, G.J. Colpas, J.W. Kampf, R.L. Brutto, W.D. Frasch, V.L. Pecoraro, Inorg. Chem. 36 (1997) 4866–4874.
[7] G.J. Colpas, B.J. Hamstra, J.W. Kampf, V.L. Pecoraro, J. Am. Chem. Soc. 116 (1994) 3627–3628.
[8] B.J. Hamstra, G.J. Colpas, V.L. Pecoraro, Inorg. Chem. 37 (1998) 949–955.
[9] J.A. Littlechild, E. Garcia–Rodriguez, Coord. Chem. Rev. 237 (2003) 65–76.
[10] G.J. Colpas, B.J. Hamstra, J.W. Kampf, V.L. Pecoraro, J. Am. Chem. Soc. 118 (1996) 3469–3478.
[11] M.R. Maurya, A. Kumar, M. Ebel, D. Rehder, Inorg. Chem. 45 (2006) 5924–5937.
[12] M.R. Maurya, A. Arya, U. Kumar, A. Kumar, F. Avecilla, J. Costa Pessoa, Dalton Trans. (2009) 9555–9566.
[13] M.R. Maurya, A.A. Khan, A. Azam, S. Ranjan, N. Mondal, A. Kumar, F. Avecilla, J. Costa Pessoa, Dalton Trans. (2010) 1345–1360.
[14] M.R. Maurya, A. Arya, A. Kumar, M.L. Kuznetsov, F. Avecilla, J. Costa Pessoa, Inorg. Chem. 49 (2010) 6586–6600.
[15] M.R. Maurya, A.K. Chandrakar, S. Chand, J. Mol. Catal. A: Chem. 263 (2007) 227–237.
[16] C. Bowers, P.K. Dutta, J. Catal. 122 (1990) 127–279.
[17] R. Raja, P. Ratnasamy, Appl. Catal.: Gen. 143 (1996) 145–158.
[18] A. Kozlov, K. Asakura, Y. Iwasawa, J. Chem. Soc., Faraday Trans. 94 (1998) 809–816.
[19] C.R. Jacob, S.P. Varkey, P. Ratnasamy, Appl. Catal.: Gen. 182 (1999) 91–96.
[20] T. Joseph, D. Srinivas, C.S. Gopinath, S.B. Halligudi, Catal. Lett. 83 (2002) 209–214.
[21] A.P.A. Marques, E.R. Dockal, F.C. Skrobot, I.L.V. Rosa, Inorg. Chem. Commun. 10 (2007) 255–261.
[22] M.R. Maurya, A.K. Chandrakar, S. Chand, J. Mol. Catal. A: Chem. 270 (2007) 225–235.
[23] M. Salavati-Niasari, M. Shaterian, M.R. Ganjali, P. Norouzi, J. Mol. Catal. A: Chem. 261 (2007) 147–155.
[24] M. Salavati-Niasari, J. Mol. Catal. A: Chem. 283 (2008) 120–128.
[25] M. Salavati-Niasari, A. Sobhani, J. Mol. Catal. A: Chem. 285 (2008) 58–67.
[26] R.A. Rowe, M.M. Jones, Inorg. Synth. 5 (1957) 113–116.
[27] R.L. Dutta, A. Syamal, Elements of Magnetochemistry, 2nd ed., Affiliated East-West Press, New Delhi, 1993, p. 8.
[28] (a) Sheldrick, G.M. SHELXS-97: An Integrated System for Solving Crystal Strucutres from Diffraction Data (Revision 5.1); University of Göttingen, Germany, 1997; (b) Sheldrick, G.M. SHELXL-86: An Integrated System for Refining Crystal Strucutres from Diffraction Data (Revision 5.1); University of Göttingen, Germany, 1993.
[29] M.R. Maurya, S. Agarwal, C. Bader, D. Rehder, Eur. J. Inorg. Chem. (2005) 147–157.
[30] F. Avecilla, P. Adão, I. Correia, J. Costa Pessoa, Pure Appl. Chem. 81 (2009) 1297–1311.
[31] M.R. Maurya, Coord. Chem. Rev. 237 (2003) 163–181.
[32] D. Rehder, C. Weidemann, A. Duch, W. Priebsch, Inorg. Chem. 27 (1988) 584–587.
[33] D. Rehder, in: S. Pregosin (Ed.), Transition Metal Nuclear Magnetic Resonance, Elsevier, New York, 1991, p. 1.
[34] V. Hulea, E. Dumitriu, Appl. Catal. A: Gen. 277 (2004) 99–106.
[35] M.R. Maurya, U. Kumar, P. Manikandan, Dalton Trans. (2006) 2575–3561.
[36] M.R. Maurya, M. Kumar, U. Kumar, J. Mol. Catal. A: Chem. 273 (2007) 133–143.
[37] H.B. ten Brink, H.E. Schoemaker, R. Wever, Eur. J. Biochem. 268 (2001) 132–138.
[38] A.G.J. Ligtenbarg, R. Hage, B.L. Feringa, Coord. Chem. Rev. 237 (2003) 89–101.
[39] P. Adão, J. Costa Pessoa, R.T. Henriques, M.L. Kuznetsov, F. Avecilla, M.R. Maurya, U. Kumar, I. Correia, Inorg. Chem. 48 (2009) 3542–3561.